


RESEARCH PAPER



Platelet-rich plasma attenuates intervertebral disc degeneration via delivering miR-141-3p-containing exosomes

Jiayuan Xu^a, Guangying Xie^b, Weiliang Yang^a, Wantao Wang^a, Zhuan Zuo^a, and Wenbo Wang ^a

^aDepartment of Orthopaedics, The First Affiliated Hospital of Harbin Medical University, Harbin, China; ^bDepartment of Blood Transfusion, The First Affiliated Hospital of Harbin Medical University, Harbin, China

ABSTRACT

Oxidative stress mediated apoptotic and pyroptotic cell death contributes to intervertebral disc (IVD) degeneration, and platelet-rich plasma (PRP) exerts protective effects to attenuate IVD degeneration. Hence, the present study aimed to validate this issue and uncover the potential underlying mechanisms. The mice and cellular models for IVD degeneration were established by using puncture method and H₂O₂ exposure, respectively, and we evidenced that NLRP3-mediated cell pyroptosis, apoptosis and inflammatory responses occurred during IVD degeneration progression *in vitro* and *in vivo*. Then, the PRP-derived exosomes (PRP-exo) were isolated and purified, and we noticed that both PRP-exo and ROS scavenger (NAC) reversed the detrimental effects of H₂O₂ treatment on the nucleus pulposus (NP) cells. Further results supported that PRP-exo exerted its protective effects on H₂O₂ treated NP cells by modulating the Keap1-Nrf2 pathway. Mechanistically, PRP-exo downregulated Keap1, resulting in the release of Nrf2 from the Keap1-Nrf2 complex, which further translocated from cytoplasm to nucleus to achieve its anti-oxidant biological functions, and H₂O₂ treated NP cells with Nrf2-deficiency did not respond to PRP-exo treatment. In addition, miR-141-3p was enriched in PRP-exo, and miR-141-3p targeted the 3' untranslated region (3'UTR) of Keap1 mRNA for its degradation, leading to Nrf2 translocation. Furthermore, overexpression of miR-141-3p ameliorated the cytotoxic effects of H₂O₂ on NP cells, which were abrogated by upregulating Keap1 and silencing Nrf2. Taken together, we concluded that PRP secreted exosomal miR-141-3p to activate the Keap1-Nrf2 pathway, which helped to slow down IVD degeneration.

ARTICLE HISTORY

Received 27 February 2021
Revised 7 June 2021
Accepted 27 June 2021

KEYWORDS

Oxidative stress;
intervertebral disc
degeneration; exosomes;
nucleus pulposus; Keap1-
Nrf2 pathway

Introduction

Intervertebral disc (IVD) degeneration is considered to be closely associated with aging and various environmental stresses, including nutrient deprivation, acidic stress, hyperglycemia, hypoxia, Reactive Oxygen Species (ROS), chronic inflammation [1–3], and the center of the disc contains a highly hydrated gelatinous aggrecan-rich core, which is also known as nucleus pulposus (NP) [1,4,5]. NP is surrounded by the annulus fibrosus (AF) containing collagen I-rich fibrous cartilage, and the boundary between NP and AF becomes obscure when IVD degeneration occurs [1,4,5]. Recently, emerging evidences pinpoint that platelet-rich plasma (PRP) can be used as therapeutic agent to attenuate IVD degeneration [6–8], but the molecular mechanisms are still largely unknown. Exosomes are a kind of vesicles with 40–100 nm

diameter, which contain cell-derived proteins, peptides and RNAs [9,10], and the existed data show that PRP-derived exosomes (PRP-exo) are critical to cure multiple diseases, such as osteoarthritis [11], diabetes [12], osteonecrosis [13], and so on. However, it is still unclear whether PRP exerts its therapeutic effects on IVD degeneration via transferring exosomes.

Cell pyroptosis is a newly identified type of inflammation-associated cell death, which is often accompanied by various pro-inflammatory cytokines secretion [14,15]. According to the previous studies, NLRP3-mediated pyroptotic cell death [16,17] and cellular inflammation [18,19] in NP cells contribute to the pathogenesis of IVD degeneration, hence, blockage of cell pyroptosis and inflammation is effective to ameliorate IVD degeneration [16–19]. Specifically, Zhang et al. verify

that mesenchymal stem cells-derived exosomes reverse IVD degeneration by inhibiting pyroptosis [17], and data from Wang et al. evidence that acacetin suppresses cellular inflammation in NP cells to slow down IVD degeneration [20]. Although no literatures reports the regulating effects of PRP on cell pyroptosis, some researchers notice the involvement of PRP and its exosomes [21] in regulating inflammatory reactions [22,23], which convince us to investigate the regulating effects of PRP-exo on cell pyroptosis and inflammation in IVD degeneration.

Oxidative stress-induced cell damages is relevant to IVD degeneration, which suppresses cell proliferation and promotes cell death in NP cells [5,24,25]. Also, oxidative stress triggers pyroptotic cell death to aggravate the development of renal ischemia-reperfusion injury [26], osteogenic dysfunction [27] and cerebral ischemia-induced neuronal injury [28]. Among all the signaling pathways, the Kelch-line ECH-associated protein 1 (Keap1)-Nuclear factor (erythroid-derived-2)-like 2 (Nrf2) pathway has been especially identified to be critical for regulating oxidative stress [29,30], cell pyroptosis [26,31] and inflammation [32]. Mechanistically, Nrf2 is released from the Keap1-Nrf2 complex under oxidative stress, which subsequently translocate from cytoplasm to nucleus to exert its anti-oxidant effects, resulting in the maintenance of cellular homeostasis [29,30]. Interestingly, Shafik et al. report that PRP modulate Nrf2 in arthritis [33], and our preliminary data verified that miR-141-3p was enriched in PRP-exo, which was confirmed as upstream regulator for Keap1 by Zhang et al. in the vascular smooth muscle cells [34].

Therefore, we conducted this work based on the published information and publications, and this study managed to uncover the potential underlying mechanisms and provide evidences to validate the utilization and feasibility of PRP-exo for IVD degeneration treatment.

Materials and methods

IVD degeneration animal models

The animal models were established by using a puncture method as previously described [35].

Briefly, the male C57BL/6 J mice (n = 12, aged 3 months old) were purchased from Research Animal Center of Harbin Medical University and were maintained in the standard specific-pathogen-free (SPF) conditions, ad libitum. The mice were anesthetized by injecting 2,2,2-tri-bromoethanol at the concentration of 125 mg/kg, and a 29-gauge needle was utilized to generate puncture at C9-C10 caudal discs, which were collected for further analysis at 6 weeks post-puncture. In addition, the mice serum was also harvested, and the C9-C10 caudal discs specimens and mice serum were stored at -70°C conditions for Real-Time qPCR, Western Blot and ELISA analysis. Our animal experiments were reviewed, monitored and approved by the Animal Ethics Committee of Harbin Medical University Affiliated First Hospital (No. 2,021,013).

Cell isolation, culture and treatment

According to the protocols provided by the previous work [35], the NP cells were isolated from the mice lumbar discs. Specifically, the resected spinal columns were used for lumbar IVDs separation, and a dissection microscope was employed to obtain AF, which were further treated with 0.1% collagenase for 3 h, and the NP tissues were acquired and primarily cultured in the DMEM/F12 medium (Gibco, USA) containing 10% fetal bovine serum (Gibco, USA) for 7 days in an incubator with 5% CO_2 humidified atmosphere and 37°C temperature. Then, the migrated NP cells were allowed to grow to form confluence, and 1 mM of the 0.25% trypsin-EDTA solution was added to collect the primary-passage NP cells, and the NP cells at passage 2 were used for further experiments. To establish the cellular models for IVD degeneration, the NP cells were exposed to 400 μM of H_2O_2 for 6 h based on our preliminary experiments (data not shown), and 50 $\mu\text{g}/\text{mL}$ of PRP-Exos and ROS scavenger (NAC, 50 mM) were incubated with the NP cells for 2 h. In addition, we purchased the HEK293T cells from ATCC (USA), which were maintained in the DMEM medium (Gibco, USA) with 10% FBS (Gibco, USA) under the standard culture conditions.

Vectors transfection

The miR-141-3p mimic, Keap1 overexpression vectors and Nrf2 knockdown vectors were designed and synthesized by a commercial third-party company (Sangon Biotech, USA), which were delivered into the NP cells by using the Lipofectamine Transfection Reagent (Invitrogen, USA) in keeping with its instructions, and the transfection efficiency was measured by using the following Real-Time qPCR analysis. The sequences for the above vectors could be found in the previous publications [29,30,36].

Analysis of real-time qPCR

Trizol reagent (Invitrogen, USA) was used to extract the total RNA from the NP cells and tissues, which were quantified spectrophotometrically at 160 nm. Then, the total RNA were reversely transcribed by the PromerScript RT Master Mix (Takara, Japan) in keeping with the producer's protocols. Finally, the Real-Time qPCR primer sequences for Keap1, Nrf2, miR-141-3p, IL-1 β , IL-18, TGF- β and IL-6 were synthesized according to the previous work [29,30,36], and the SYBR premix Ex Taq (Takara, Japan) combined with a Step One Plus PCR system (Applied Biosystems, USA) were performed for miRNA and mRNA quantification, which were respectively normalized by their internal inference U6 and β -actin.

Protein quantification by Western blot analysis

According to the protocols provided by the previous study [35], we segregated the nucleus and cytoplasm of the NP cells by using the extraction buffer and subsequent centrifugation (600 g, 10 min, 4°C). Then, the proteins were obtained from the NP cells (cytoplasm/nucleus) and tissues by using the RIPA lysis buffer (Beyotime, Shanghai, China), and the protein concentration was measured by BCA kit (Beyotime, Shanghai, China). Next, the proteins were separated by 10% SDS-PAGE, and were transferred onto the PVDF membranes (Millipore, USA), which were blocked by 5% nonfat milk and were sequentially

incubated with the primary antibodies against NLRP3 (1:1500, Abcam, UK), Gasdermin D (1:2000, Abcam, UK), β -actin (1:2000, Abcam, UK), Keap1 (1:1000, Abcam, UK) and Nrf2 (1:2000, Abcam, UK), and with the secondary antibodies (1:3000, Proteintech, USA). Finally, the protein bands were visualized by ECL system (Bio-Rad, USA) and were quantified by Image J software.

Enzyme-linked immunosorbent assay (ELISA)

The expression levels of the pro-inflammatory cytokines (IL-1 β , IL-18, TGF- β and IL-6) in the NP cell supernatants and mice serum were measured by their corresponding ELISA kit (Abcam, UK) according to the manufacturer's protocol. Briefly, the NP cells' supernatants were collected and homogenized by using the TBST buffer with 0.1 Tween 20 supplementation. Then, the supernatants were subjected to 13,000 g centrifugation for 5 min, and were collected for quantification of the inflammatory cytokines.

Examination of ROS levels

The NP cells were subjected to H₂O₂ treatment, and the Reactive Oxygen Species Assay Kit (YEASEN, Shanghai, China) was bought to examine ROS levels in the NP cells in keeping with the manufacturer's instructions. The NP cells were incubated with 2, 7-Dichlorodi-hydrofluorescein diacetate (DCFH-DA) working solution for 30 min at 37°C without light exposure, and the extracellular DCFH-DA probes were washed away by using the PBS buffer for 3 times. Next, we used a fluorescence microscope (ThermoFisher Scientific, USA) to observe and photograph the fluorescent images, which were further analyzed by Image J software to evaluate ROS generation. In addition, the GSH/GSSG Ratio Detection Assay Kit (Fluorometric - Green) (ab138881, Abcam, UK) was used to examine GSH/GSSG Ratio in the NP cells by a fluorescence microplate reader at Ex/Em = 490/520 nm in keeping with the producer's instructions.

Flow cytometer (FCM) for cell apoptosis

The Apoptosis Detection Kit (YEASEN, Shanghai, China) was used to examine cell apoptosis according to the manufacturer's protocol. In brief, the NP cells were respectively stained with Annexin V-FITC and Propidium iodide (PI) for 10–15 min at room temperature in darkness. Then, the cells were suspended by $1 \times$ binding buffer on ice, and the cell apoptosis ratio was examined by a flow cytometer (BD Bioscience, USA).

Examination of cell proliferation and viability

We respectively conducted MTT assay and trypan blue staining assay to measure cell proliferation and viability in NP cells. Specifically, the NP cells in passage 2 were seeded in the 96-well plates, which were subsequently subjected to differential treatments, and were incubated with MTT solution for 2 h. Then, the formed formazan was dissolved by the DMSO solution, and the 96-well plates were fully vortexed and the optical density (OD) values were measured by a microplate reader (ThermoFisher Scientific, USA) to evaluate cell proliferation. Moreover, the NP cells were stained with trypan blue solution for 15 min at 37°C, and the dead blue cells were counted to evaluate cell viability under a light microscope (ThermoFisher Scientific, USA).

Dual-luciferase reporter gene system assay

The dual-luciferase reporter gene system assay were performed according to the published experimental protocols [37,38]. Specifically, we predicted the targeting sites of miR-141-3p and Keap1 mRNA by using the online starBase software (<http://starbase.sysu.edu.cn/>), and the predicted binding sequences in Keap1 were mutated and cloned into the luciferase reporter provided by Sangon Biotech (Shanghai, China), and the wild-type and mutated Keap1 were named as Wt-Keap1 and Mut-Keap1, respectively. Then, the miR-141-3p mimic and Keap1 luciferase reporter vectors were co-transfected into the HEK293T cells, and the luciferase activities were measured by using a luciferase detection kit (Beyotime, Shanghai, China).

RNA pull-down assay

The binding abilities of miR-141-3p and Keap1 mRNA were verified by the following RNA pull-down assay in keeping with the protocols reported in the previous work [39]. Firstly, the biotin-labeled 3' UTR of Keap1 mRNA was designed and synthesized by Sangon Biotech (Shanghai, China), which were used for further pull-down assay. The NP cells were fixed, lysed and centrifuged, and the supernatants were collected as input. Next, the Keap1 probes were incubated with the lysates overnight at room temperature, and formaldehyde crosslinking was reversed by Proteinase K. Finally, Real-Time qPCR was conducted to measure the enrichment of miR-141-3p by Keap1 probes.

Data collection, analysis and visualization

The data were presented as Means \pm Standard Deviations (SD), and were analyzed by SPSS 18.0 software. Means from two groups were compared by the Student's t-test, and one-way ANOVA analysis combined with its post-hoc correction method (Tukey post-hoc test) was conducted for the comparisons of means from multiple groups. Finally, the data were visualized by GraphPad Prism 8.0 software. Each experiment had at least 3 repetitions, and $*P < 0.05$ was statistical significance.

Results

Establishment of IVD degeneration models *in vitro* and *in vivo*

Initially, according to the previous work [35], we established the mice models for IVD degeneration by using the puncture method, and the IVD sections were collected for further analysis. As shown in (Figure 1(a,b)), the expression levels of pyroptosis associated biomarkers (NLRP3, cleaved Gasdermin D and caspase-1) were significantly increased in the mice tissues with IVD degeneration, in contrast with their normal counterparts. In addition, by performing the Real-Time qPCR analysis, we noticed that the mRNA levels of IL-1 β , IL-18, TGF- β and IL-6 were increased in IVD degeneration mice (Figure 1(c)). Consistently, the

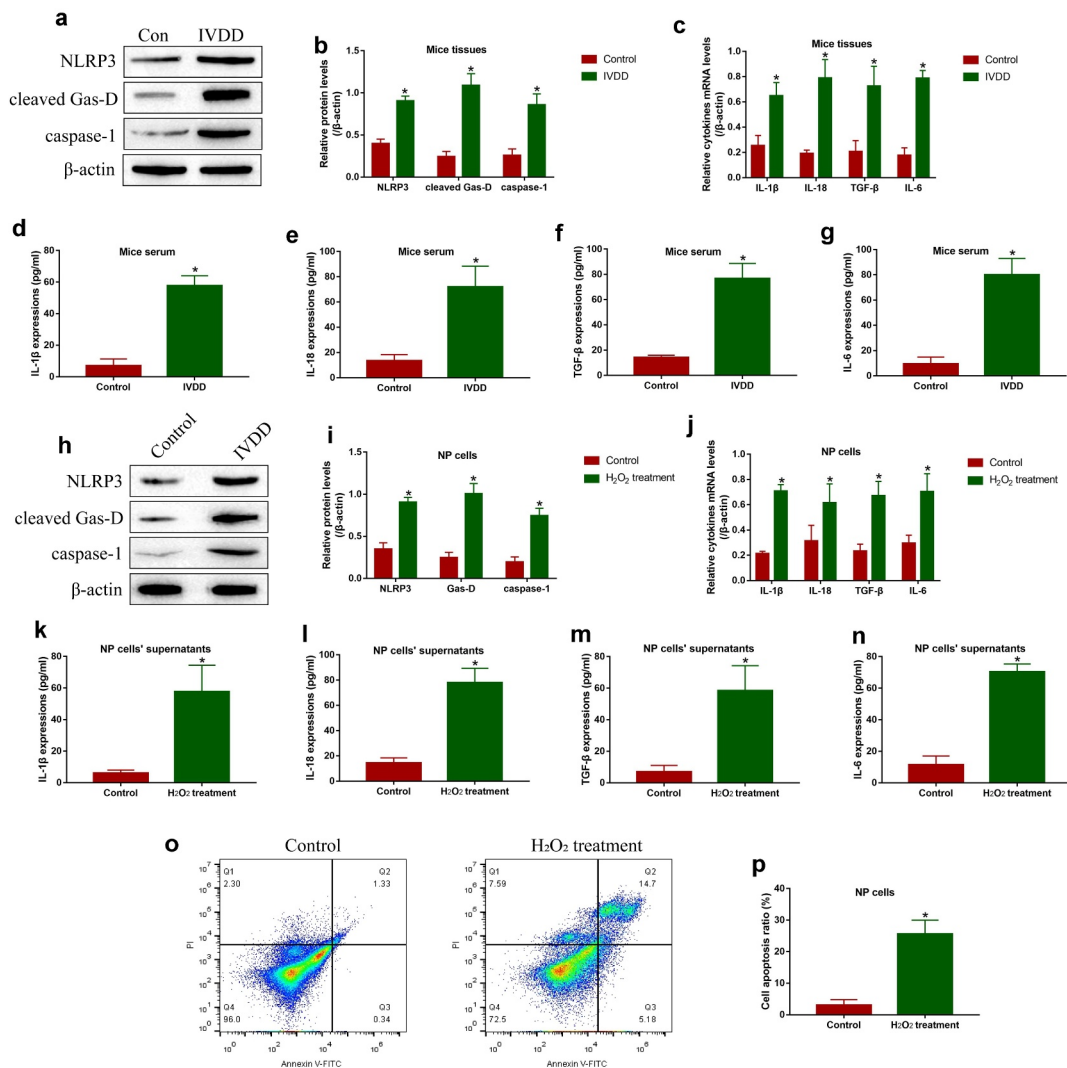


Figure 1. Cell pyroptosis and inflammation involved in regulating IVD degeneration. The mice IVD tissues were collected, and (a, b) Western Blot analysis was performed to examine NLRP3, cleaved Gasdermin D and caspase-1 expressions. The (c) mRNA levels in IVD tissues and (d-g) secretion of the pro-inflammatory cytokines in mice serum were detected by Real-Time qPCR and ELISA. The NP cells were subjected to H₂O₂ treatment, and (h, i) NLRP3, cleaved Gasdermin D and caspase-1 were examined by Western Blot, and (j) Real-Time qPCR and (k-n) ELISA were respectively used to measure the generation and secretion of the pro-inflammatory cytokines. (o, p) The NP cells were double-stained with Annexin V-FITC and PI, and FCM was performed to examine cell apoptosis ratio. * $P < 0.05$ was deemed as statistical significance.

ELISA results supported that IL-1 β (Figure 1(d)), IL-18 (Figure 1(e)), TGF- β (Figure 1(f)) and IL-6 (Figure 1(g)) were also upregulated in mice serum with IVD degeneration. Moreover, the NP cells were exposed to H₂O₂ treatment to mimic the realistic conditions of IVD degeneration *in vitro*, and the data in (Figure 1(h,i)) showed that H₂O₂ upregulated NLRP3, cleaved Gasdermin D and caspase-1 to trigger pyroptotic cell death in NP

cells, and further Real-Time qPCR (Figure 1(j)) and ELISA (Figure 1(k-n)) results evidenced that H₂O₂ also promoted IL-1 β , IL-18, TGF- β and IL-6 generation and secretion in NP cells and their supernatants. Additionally, H₂O₂ treatment promoted cell apoptosis in NP cells (Figure 1(o,p)), the above results suggested that cell pyroptosis and inflammation were closely associated with the pathogenesis of IVD degeneration.

Both PRP-exo and NAC attenuated H₂O₂ treatment-induced NP cell pyroptosis and inflammation

Based on the available information that PRP-exo is reported as an effective therapeutic agent for IVD degeneration [7,40], and NAC acts as ROS scavenger to exert its anti-oxidant effects [41]. The PRP-exo were isolated, which were further observed by electron microscope (Figure 2(a), upper panel) and were identified by Western Blot analysis with its biomarkers TSG101 and CD81 (Figure 2(a), lower panel). Next, the NP cells were treated with both PRP-exo and NAC, which were further divided into four groups, including Control, H₂O₂ alone,

H₂O₂ plus PRP-exo (H₂O₂+ PRP-exo), and H₂O₂ plus NAC (H₂O₂+ NAC) groups. Then, the cells were incubated with DCFH-DA probes, and the results showed that both PRP-exo and NAC eliminated ROS generation in NP cells treated with H₂O₂ (Figure 2(b)). Further results supported that the inhibiting effects of H₂O₂ treatments on GSH/GSSG ratio in NP cells were abrogated by both PRP-exo and NAC (Figure 2(c)). Also, we expectedly found that the promoting effects of H₂O₂ on NLRP3, cleaved Gasdermin D and caspase-1 were reversed by co-treating NP cells with PRP-exo and NAC (Figure 2(d,e)). In addition, data in (Figure 2(f-j)) supported that both PRP-exo and

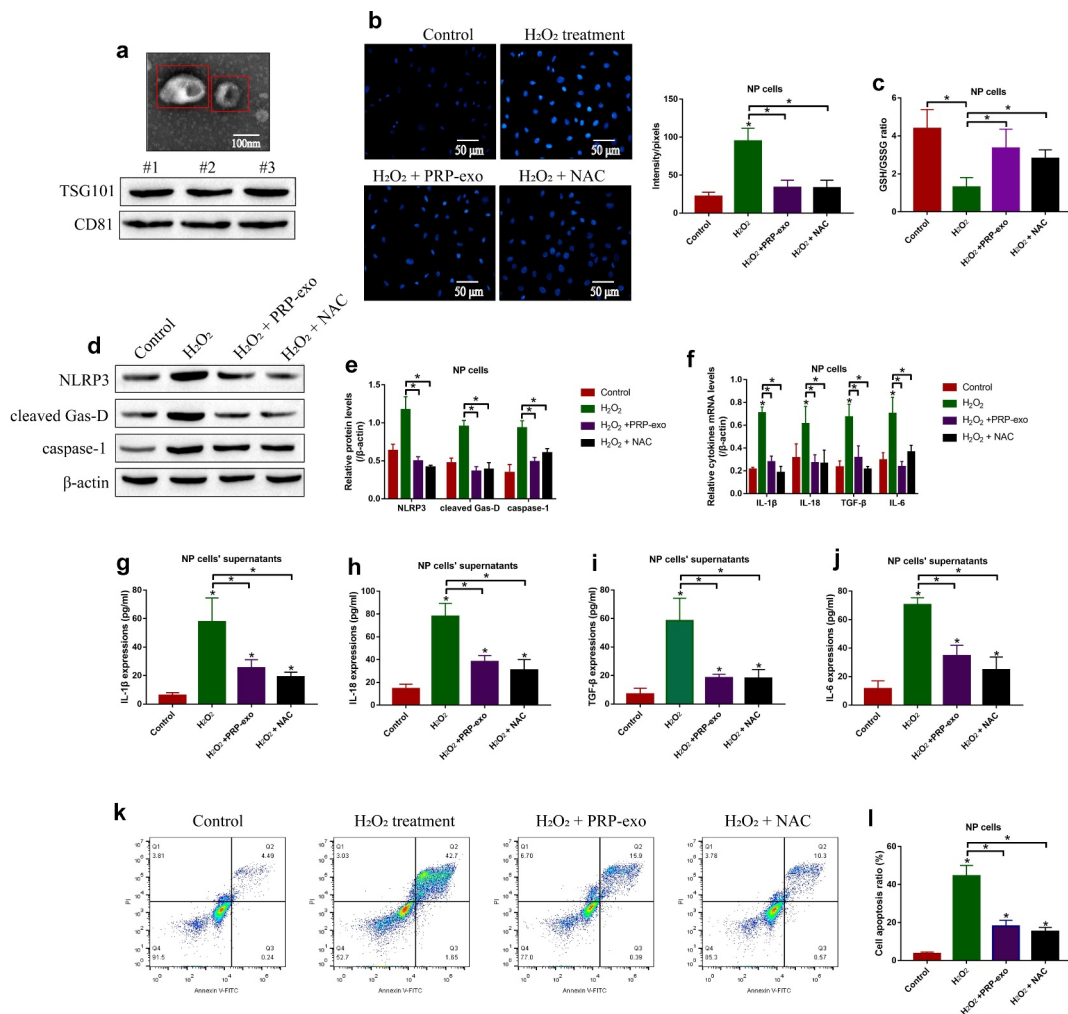


Figure 2. The reversal effects PRP-exo and NAC on H₂O₂ treated NP cells. (a) The PRP-exo was observed by electron microscope, which were subsequently identified by Western Blot analysis for its biomarkers TSG101 and CD81. (b) The NP cells were stained with DCFH-DA probes, and the fluorescent microscope was used to examine ROS density. (c) The GSH/GSSG ratio was determined in NP cells to reflect oxidative stress. (d, e) The expression status of NLRP3, cleaved Gasdermin D and caspase-1 were measured by Western Blot analysis. (f) Cytokines generation and (g-j) secretion were quantified by Real-Time qPCR and ELISA. (k, l) Annexin V-FITC/PI double staining method was performed to evaluate cell apoptosis. **P* < 0.05 was deemed as statistical significance.

NAC suppressed the pro-inflammatory cytokines (IL-1 β , IL-18, TGF- β and IL-6) generation and secretion in NP cells and their supernatants. Furthermore, the results in (Figure 2(k,l)) evidenced that PRP-exo and NAC ameliorated H₂O₂-induced cell apoptosis in NP cells. The above results suggested that H₂O₂-induced both pyroptotic and apoptotic cell death in NP cells by triggering ROS production.

The regulating effects of PRP-exo on the Keap1-Nrf2 pathway

The Keap1-Nrf2 pathway involves in regulating oxidative stress and IVD degeneration [5], and PRP-exo exerts its anti-oxidant effects to attenuate IVD degeneration [7,40]. Based on this, we investigated the effects of PRP-exo on the Keap1-Nrf2 pathway in NP cells. To achieve this, the NP cells were exposed to PRP-exo treatment, and we surprisingly found that PRP-exo downregulated Keap1 and upregulated Nrf2 in NP cells (Figure 3a-c). In addition, the nuclear and cytoplasm sections of the NP cells were obtained, and our data in (Figure 3(d-f)) showed that Nrf2 tended to be enriched in the nucleus of PRP-exo treated NP cells, which were reversed by upregulating Keap1. The above results hinted that, PRP-

exo downregulated Keap1 to release Nrf2 from Keap1-Nrf2 complex, as a result, Nrf2 translocated from cytoplasm to nucleus to exert its biological functions.

PRP-exo regulated cellular functions in the H₂O₂ treated NP cells in a Nrf2-dependent manner

To further understand whether PRP-exo sustains normal functions of H₂O₂ treated NP cells, the Nrf2 downregulation vectors were designed and transfected to establish the Nrf2-deficient NP cells (Figure S1(d, e)). By performing the MTT assay (Figure 4(a,b)) and trypan blue staining assay (Figure 4(c,d)), we expectedly found that PRP-exo rescued cell proliferation and viability in H₂O₂ treated normal NP cells, but not in the NP cells with Nrf2 knockdown. Consistently, the inhibiting effects of PRP-exo on H₂O₂-induced apoptotic cell death were also abrogated by silencing Nrf2 (Figure 4(e,f)). Moreover, the following experiments validated that PRP-exo attenuate cell pyroptosis and inflammation in a Nrf2-dependent manner (Figure 4(g-m)). Specifically, Western Blot analysis results in (Figure 4(g,h)) showed that knock-down of Nrf2 increased the expression levels of NLRP3, cleaved Gasdermin D and

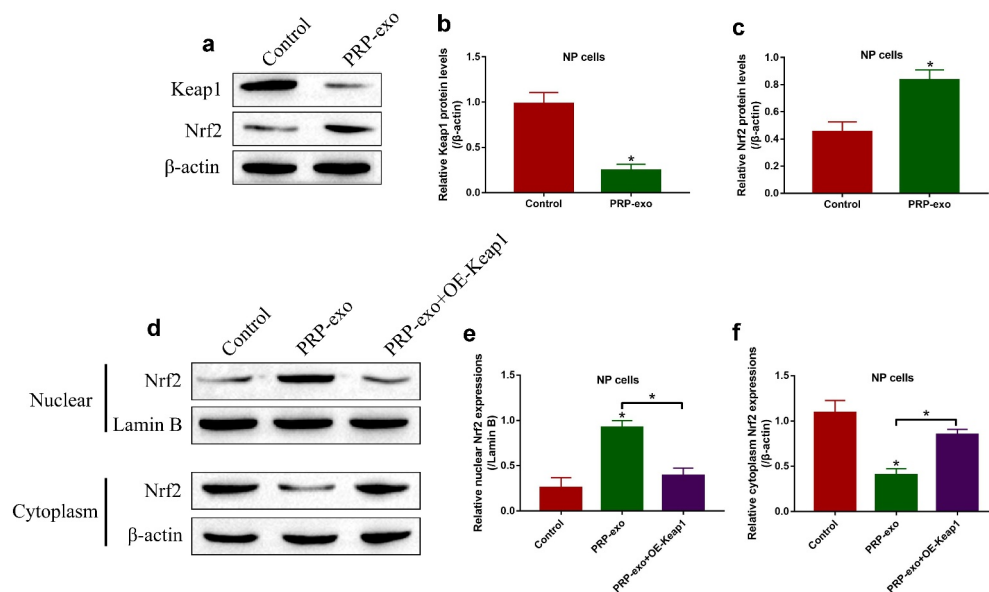


Figure 3. The regulating effects of PRP-exo on the Keap1-Nrf2 pathway in NP cells. (a-c) The expression levels of Keap1 and Nrf2, and (d-f) Nrf2 translocation from cytoplasm to nucleus were measured by using the Western Blot analysis. * $P < 0.05$ was deemed as statistical significance.

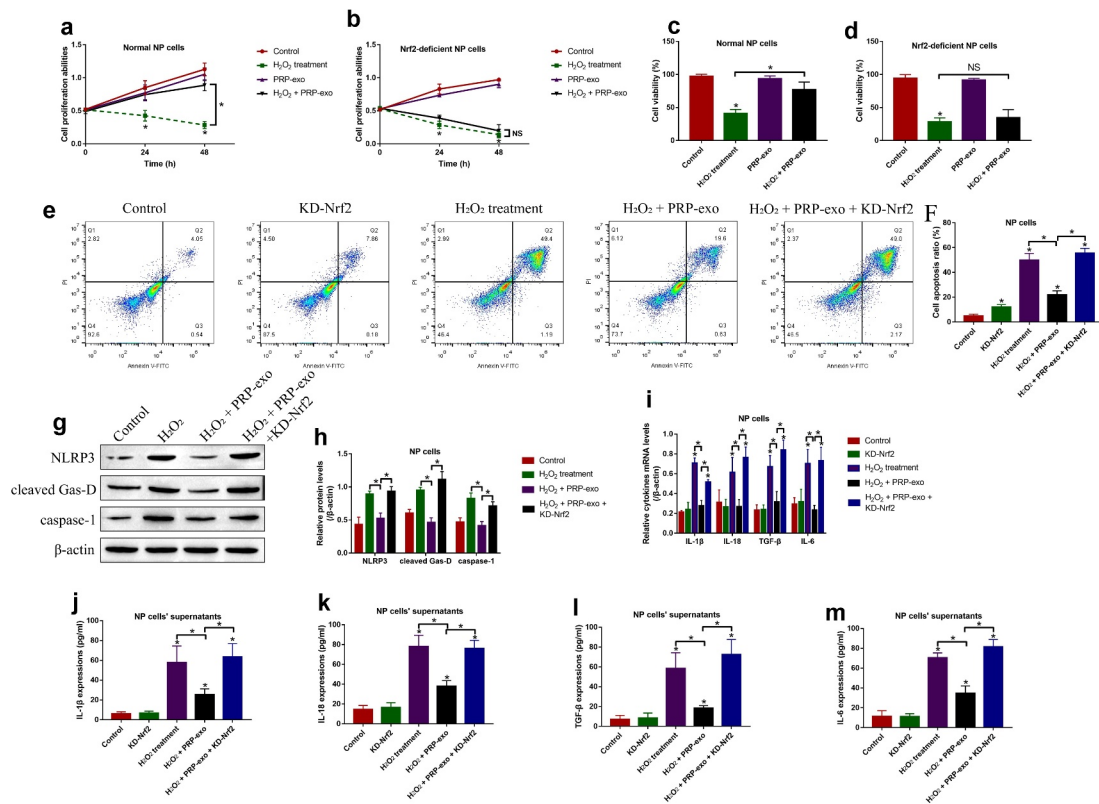


Figure 4. PRP-exo exerted its protective effects on H_2O_2 -induced NP cell death in a Nrf2-dependent manner. (a, b) Cell proliferation and (c, d) viability were respectively examined by MTT assay and trypan blue staining assay. (e, f) The FCM was performed to measure the Annexin V-FITC- or PI-positive apoptotic cells. (g, h) Quantification of NLRP3, cleaved Gasdermin D and caspase-1 by Western Blot analysis. (i) Real-Time qPCR was used to examine mRNA levels of the pro-inflammatory cytokines generation. (j-m) The protein levels of the inflammation associated cytokines in the supernatants were measured by ELISA. * $P < 0.05$ was deemed as statistical significance.

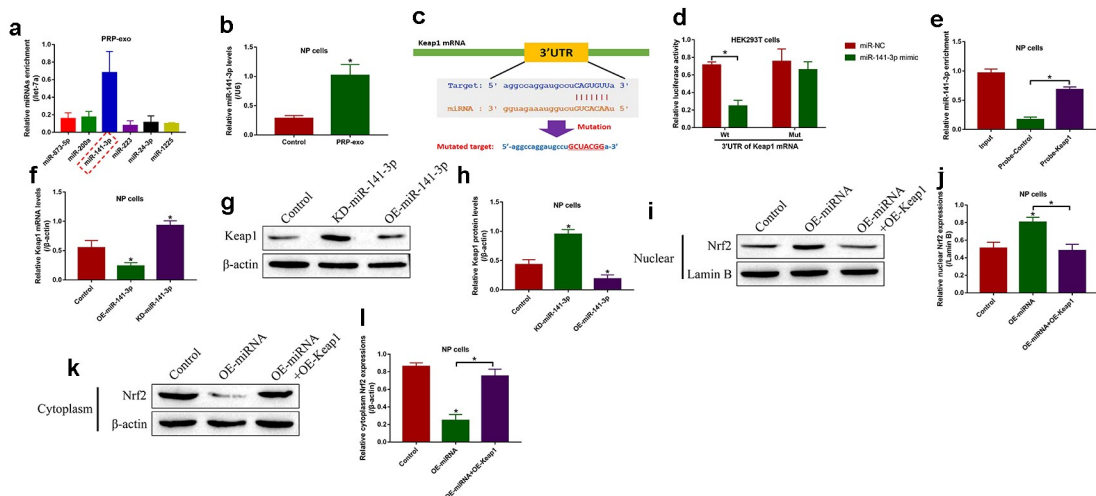


Figure 5. PRP-exo delivered exosomal miR-141-3p to modulate the Keap1/Nrf2 signaling pathway in NP cells. Real-Time qPCR was used to examine the expression levels of the upstream miRNAs for Keap1 in (a) PRP-exo, and the expression status of miR-141-3p in NP cells were also determined. (c) The targeting sites of miR-141-3p and 3'UTR of Keap1 mRNA were predicted, which were further verified by (d) dual-luciferase reporter gene system assay and (e) RNA pull-down assay. (f) The mRNA and (g, h) protein levels of Keap1 were respectively examined. (i-l) Western Blot analysis was used to analyze the Nrf2 translocation in NP cells. * $P < 0.05$ was deemed as statistical significance.

caspase-1 to aggravated cell pyroptosis in PRP-exo-H₂O₂ co-treated NP cells. Similarly, PRP-exo suppressed the generation (Figure 4(i)) and secretion (Figure 4(j-m)) of the pro-inflammatory cytokines (IL-1 β , IL-18, TGF- β and IL-6) in the PRP-exo treated NP cells, which were promoted by knocking down Nrf2.

PRP-exo regulated the Keap1-Nrf2 pathway by secreting miR-141-3p-containing exosomes

Previous studies report that PRP-exo delivered exosomal miRNAs to the target cells [34], and miRNAs act as post-transcriptional regulators to regulate the downstream genes by targeting their 3' untranslated regions (UTRs) [38]. Interestingly, we identified that miR-141-3p, instead of the other upstream regulators for Keap1, tended to be enriched in the PRP-exo (Figure 5(a)), and let-7a was used as internal inference as previously described [42]. Then, the PRP-exo was incubated with the NP cells, and we noticed that PRP-exo delivered miR-141-3p into the NP cells for its upregulation (Figure 5(b)). Next, the targeting sites in miR-141-3p and Keap1 mRNA were predicted by using the bioinformatics analysis, and the binding sites in Keap1 were mutated (Figure 5(c)). Then, the dual-luciferase reporter gene system assay validated that miR-141-3p was capable of binding to the 3'UTR of Keap1 mRNA (Figure 5(d)), and the following RNA pull-down assay results evidenced that miR-141-3p could be enriched by Keap1 probes (Figure 5(e)). Next, the miR-141-3p mimic and inhibitor were synthesized and transfected into the NP cells (Figure S1(a)), and the results supported that miR-141-3p negatively regulated Keap1 at both transcriptional (Figure 5(f)) and translational (Figure 5(g,h)) levels. Moreover, Keap1 was overexpressed in NP cells (Figure S1b, c), and the Western Blot results in (Figure 5(i-l)) validated that overexpression of miR-141-3p promoted Nrf2 translocation from cytoplasm to nucleus, which were reversed by upregulating Keap1.

Overexpression of miR-141-3p restrained H₂O₂-induced cell death and inflammation in NP cells

Next, the biological functions and mechanisms of miR-141-3p in regulating H₂O₂-induced NP cell death were investigated. To achieve this, miR-141-3p was overexpressed in the NP cells (Figure S1(a)), which were divided into four groups, including Control, H₂O₂ alone, and H₂O₂ plus OE-miR-141-3p group. As shown in (Figure 6(a,b)), the inhibiting effects of H₂O₂ treatment on cell proliferation and viability in NP cells were rescued by upregulating miR-141-3p. Consistently, the NP cells were subsequently stained with Annexin V-FITC and PI, and the following flow cytometry (FCM) results validated that the promoting effects of H₂O₂ treatment on NP cell apoptosis were attenuated by upregulating miR-141-3p (Figure 6(c,d)). Then, we performed Western Blot analysis to examine the pyroptosis-associated proteins, and found that miR-141-3p overexpression decreased the expression levels of NLRP3, cleaved Gasdermin D and caspase-1 to block cell pyroptosis in H₂O₂ treated NP cells (Figure 6(e,f)). Furthermore, the Real-Time qPCR (Figure 6(g)) and ELISA (Figure 6(h-k)) results supported that H₂O₂-induced pro-inflammatory cytokines (IL-1 β , IL-18, TGF- β and IL-6) production and secretion in NP cells were also inhibited by upregulating miR-141-3p.

Discussion

The pathogenesis of intervertebral disc (IVD) degeneration is very complicated, which is often attributed to aging and other environmental stresses [1–3]. Currently, IVD degeneration brings huge health burden as the results of its unclear progression mechanisms and a lack of effective therapeutic treatment strategies [43,44]. According to the previous publications, platelet-rich plasma (PRP) was proved to be effective for IVD degeneration treatment [6–8], and PRP-derived exosomes (PRP-exo) might be critical in this process [11–13], but the detailed mechanisms were still unclear. Based on the above information, the PRP-exo was isolated and purified in the

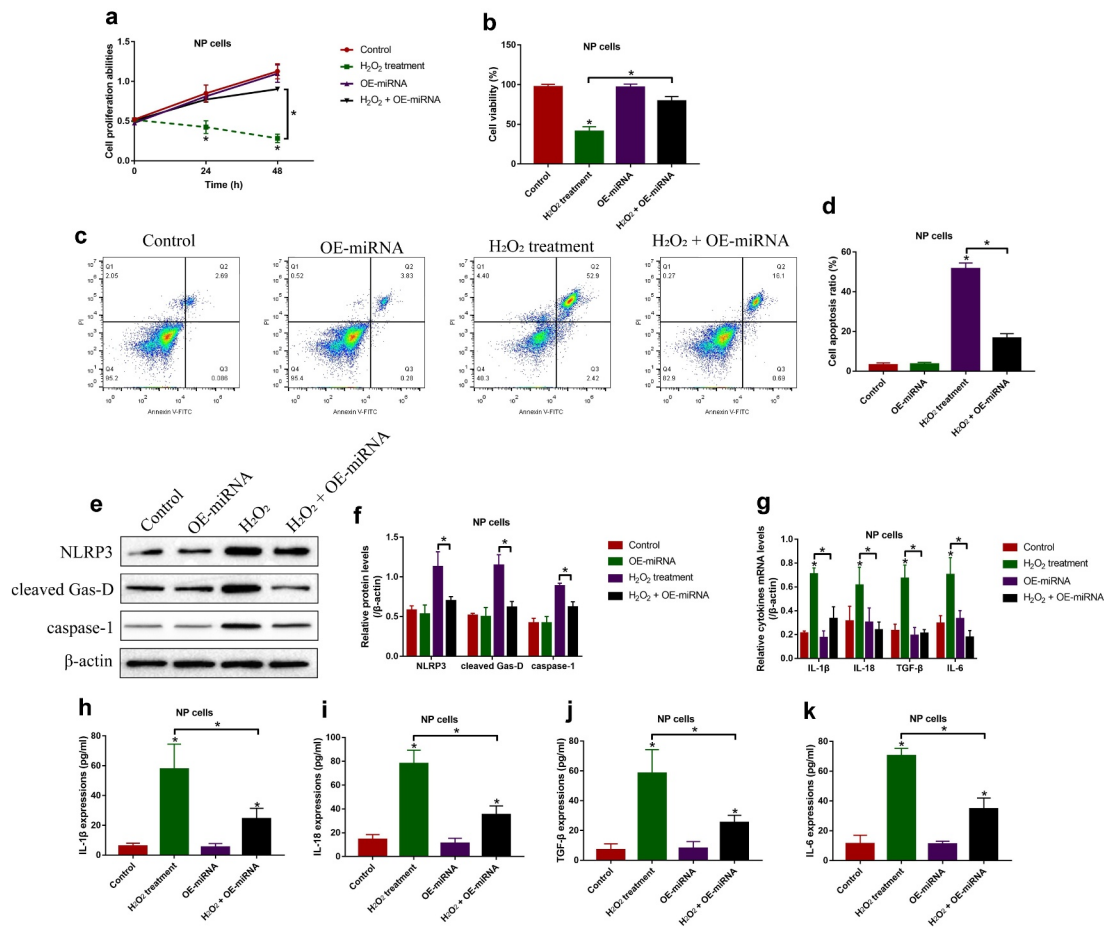


Figure 6. Overexpression of miR-141-3p attenuated H₂O₂-induced cell death in NP cells. (a) MTT assay and (b) trypan blue staining assay were used to examine cell proliferation and viability, respectively. (c, d) Cell apoptosis ratio in the NP cells was examined by FCM assay. (e, f) The expression levels of NLRP3, cleaved Gasdermin D and caspase-1 were examined by Western Blot. The expression status of the pro-inflammatory cytokines were examined by (g) Real-Time qPCR and (h-k) ELISA, respectively. **P* < 0.05 was deemed as statistical significance.

present study, and we provided evidences to support that PRP-exo were effective to ameliorate IVD degeneration *in vitro* and *in vivo*, and we also uncovered the potential underlying mechanisms that PRP-exo regulated the Keap1-Nrf2 pathway via exosomal miR-141-3p delivery.

Previous data evidenced that cell pyroptosis, apoptosis, and inflammation were closely associated with IVD degeneration [14,15,45,46], by using the reported puncture method [5], the mice models for IVD degeneration were established, and we expectedly found that NLRP3-mediated cell pyroptosis and inflammation occurred in IVD degeneration mice C9-C10 caudal discs. Consistently, the NP cells were isolated and treated with H₂O₂ to mimic the realistic conditions of IVD degeneration *in vitro*, and the data supported that H₂O₂ induced cell apoptosis, pyroptosis and

pro-inflammatory cytokines secretion in the NP cells, which were supported by the previous studies [14,15,45,46]. Given that PRP had been used for IVD degeneration treatment [6–8], and PRP-exo was considered as the main components that contributed to IVD degeneration recovery [11–13], we found that PRP-exo reversed the detrimental effects of H₂O₂ treatment on NP cells, suggesting that PRP-exo was effective to attenuate IVD degeneration *in vitro*. In addition, there existed interplays among oxidative stress, cell pyroptosis, apoptosis and inflammation [26,47], and our data validated that blockage of oxidative stress attenuated H₂O₂-induced cell apoptosis, pyroptosis and inflammation in NP cells. According to recent publications, both apoptotic and pyroptotic cell death involve in IVD degeneration [14,15,45,46], and Lamkanfi et al. evidence that caspase-8

molecular switch is pivotal for the transition between cell apoptosis and pyroptosis [48], which raised the interesting academic issue that there might exist interplays between these two types of cell death during IVD degeneration, however, this issue needed to be further investigated in our future work.

Next, we investigated the potential underlying mechanisms, and identified that the Keap1-Nrf2 pathway could be activated by PRP-exo in the NP cells. The Keap1-Nrf2 pathway is capable of regulating various cellular functions, including oxidative stress [29,30], cell pyroptosis [26,31] and inflammation [32]. Mechanistically, under the normal conditions, Keap1 combines with Nrf2 to form the Keap1-Nrf2 complex in the cytoplasm, and Nrf2 is subsequently degraded in a ubiquitination-dependent manner. Nrf2 is released from the Keap1-Nrf2 complex and translocate from the cytoplasm to nucleus when the cells experience oxidative stress, and Nrf2 initiates antioxidant response element (ARE) to exert its anti-oxidant effects and sustains cellular homeostasis [29,30], and we evidenced that PRP-exo inhibited Nrf2 degradation and promoted its translocation, and downregulated Keap1 in the NP cells, which were partially in consistent with the previous data [29,30] and convinced us to investigate the mechanisms by which PRP-exo suppressed Keap1 to facilitate Nrf2 translocation. Through Real-Time qPCR screening analysis, we noticed one of the the upstream regulators of Keap1, miR-141-3p, was enriched and could be transferred by PRP-exo to the NP cells for its upregulation. Further data evidenced that overexpression of miR-141-3p exerted protective effects to reverse H₂O₂-induced cell pyroptosis, apoptosis and inflammation in NP cells. Nevertheless, since the pathogenesis of IVD degeneration was complicated, future RNA-seq analysis was still needed to identify novel diagnostic and therapeutic biomarkers for this disease [49–51].

Conclusions

In general, PRP-exo delivered miR-141-3p to degrade Keap1, leading to the release of Nrf2 from the Keap1-Nrf2 complex, which further translocated from cytoplasm to nucleus to exert its anti-oxidant

effects, resulting in the inhibition of oxidative stress-mediated cell pyroptosis and attenuate IVD degeneration. Although our data was solid to support our current conclusions, the clinical specimens were needed to be collected to validate our preliminary experiments in clinic in our future work.

Disclosure statement

No potential conflict of interest was reported by the author(s).

Consent for publications

All the co-authors agreed to publish the final version of this manuscript.

Ethics approval and consent to participate

All the Animal Ethics Committee of Harbin Medical University Affiliated First Hospital (No. 2,021,013).

Availability of data and material

All the data had been included in the manuscript, and the raw data for this work could be obtained from the corresponding author upon reasonable request.

ORCID

Wenbo Wang  <http://orcid.org/0000-0001-5501-1039>

References

- [1] Li Z, Chen X, Xu D, et al. Circular RNAs in nucleus pulposus cell function and intervertebral disc degeneration. *Cell Prolif.* 2019;52(6):e12704.
- [2] Silva MJ, Holguin N. Aging aggravates intervertebral disc degeneration by regulating transcription factors toward chondrogenesis. *The FASEB Journal.* 2020;34(2):1970–1982.
- [3] Yurube T, Ito M, Kakiuchi Y, et al. Autophagy and mTOR signaling during intervertebral disc aging and degeneration. *JOR Spine.* 2020;3(1):e1082.
- [4] Liao Z, Luo R, Li G, et al. Exosomes from mesenchymal stem cells modulate endoplasmic reticulum stress to protect against nucleus pulposus cell death and ameliorate intervertebral disc degeneration in vivo. *Theranostics.* 2019;9(14):4084–4100.
- [5] Tang Z, Hu B, Zang F, et al. Nrf2 drives oxidative stress-induced autophagy in nucleus pulposus cells via a Keap1/Nrf2/p62 feedback loop to protect

- intervertebral disc from degeneration. *Cell Death Dis.* **2019**;10(7):510.
- [6] Gelalis ID, Christoforou G, Charchanti A, et al. Autologous platelet-rich plasma (PRP) effect on intervertebral disc restoration: an experimental rabbit model. *Eur J Orthop Surg Traumatol.* **2019**;29(3):545–551.
- [7] Chang Y, Yang M, Ke S, et al. Effect of platelet-rich plasma on intervertebral disc degeneration in vivo and in vitro: a critical review. *Oxid Med Cell Longev.* **2020**;8893819. DOI:10.1155/2020/8893819
- [8] Choi MH, Blanco A, Stealey S, et al. Micro-clotting of platelet-rich plasma upon loading in hydrogel microspheres leads to prolonged protein release and slower microsphere degradation. *Polym (Basel).* **2020**;12(8). DOI: 10.3390/polym12081712.
- [9] Gurunathan S, Kang M-H, Jeyaraj M, et al. Review of the isolation, characterization, biological function, and multifarious therapeutic approaches of exosomes. *Cells.* **2019**;8(4):307.
- [10] Qin W, Dallas SL. Exosomes and extracellular RNA in muscle and bone aging and crosstalk. *Curr Osteoporos Rep.* **2019**;17(6):548–559.
- [11] Liu X, Wang L, Ma C, et al. Exosomes derived from platelet-rich plasma present a novel potential in alleviating knee osteoarthritis by promoting proliferation and inhibiting apoptosis of chondrocyte via Wnt/ β -catenin signaling pathway. *J Orthop Surg Res.* **2019**;14(1):470.
- [12] Guo SC, Tao SC, Yin WJ, et al. Exosomes derived from platelet-rich plasma promote the re-epithelization of chronic cutaneous wounds via activation of YAP in a diabetic rat model. *Theranostics.* **2017**;7(1):81–96.
- [13] Tao S-C, Yuan T, Rui B-Y, et al. Exosomes derived from human platelet-rich plasma prevent apoptosis induced by glucocorticoid-associated endoplasmic reticulum stress in rat osteonecrosis of the femoral head via the Akt/Bad/Bcl-2 signal pathway. *Theranostics.* **2017**;7(3):733–750.
- [14] Van Opdenbosch N, Lamkanfi M. Caspases in cell death, inflammation, and disease. *Immunity.* **2019**;50(6):1352–1364.
- [15] Broz P, Pelegrín P, Shao F. The gasdermins, a protein family executing cell death and inflammation. *Nat Rev Immunol.* **2020**;20(3):143–157.
- [16] He D, Zhou M, Bai Z, et al. Propionibacterium acnes induces intervertebral disc degeneration by promoting nucleus pulposus cell pyroptosis via NLRP3-dependent pathway. *Biochem Biophys Res Commun.* **2020**;526(3):772–779.
- [17] Zhang J, Zhang J, Zhang Y, et al. Mesenchymal stem cells-derived exosomes ameliorate intervertebral disc degeneration through inhibiting pyroptosis. *J Cell Mol Med.* **2020**;24(20):11742–11754.
- [18] Dong W, Liu J, Lv Y, et al. miR-640 aggravates intervertebral disc degeneration via NF- κ B and WNT signalling pathway. *Cell Prolif.* **2019**;52(5):e12664.
- [19] Zhang Y, He F, Chen Z, et al. Melatonin modulates IL-1 β -induced extracellular matrix remodeling in human nucleus pulposus cells and attenuates rat intervertebral disc degeneration and inflammation. *Aging (Albany NY).* **2019**;11(22):10499–10512.
- [20] Wang H, Jiang Z, Pang Z, et al. Acacetin alleviates inflammation and matrix degradation in nucleus pulposus cells and ameliorates intervertebral disc degeneration in vivo. *Drug Des Devel Ther.* **2020**;14:4801–4813.
- [21] Zhang W, Dong X, Wang T, et al. Exosomes derived from platelet-rich plasma mediate hyperglycemia-induced retinal endothelial injury via targeting the TLR4 signaling pathway. *Exp Eye Res.* **2019**;189:107813.
- [22] O'Donnell C, Migliore E, Grandi FC, et al. Platelet-rich plasma (PRP) from older males with knee osteoarthritis depresses chondrocyte metabolism and upregulates inflammation. *J Orthop Res.* **2019**;37(8):1760–1770.
- [23] Belebecha V, Casagrande R, Urbano MR, et al. Effect of the platelet-rich plasma covering of polypropylene mesh on oxidative stress, inflammation, and adhesions. *Int Urogynecol J.* **2020**;31(1):139–147.
- [24] Che H, Li J, Li Y, et al. p16 deficiency attenuates intervertebral disc degeneration by adjusting oxidative stress and nucleus pulposus cell cycle. Vol. 9, *Elife*; **2020**. ENGLAND: eLife Sciences Publications.
- [25] Zhang G-Z, Deng Y-J, Xie -Q-Q, et al. Sirtuins and intervertebral disc degeneration: roles in inflammation, oxidative stress, and mitochondrial function. *Clin Chim Acta.* **2020**;508:33–42.
- [26] Diao C, Chen Z, Qiu T, et al. Inhibition of PRMT5 attenuates oxidative stress-induced pyroptosis via activation of the Nrf2/HO-1 Signal pathway in a mouse model of renal ischemia-reperfusion injury. *Oxid Med Cell Longev.* **2019**;2345658. DOI:10.1155/2019/2345658
- [27] Liu S, Du J, Li D, et al. Oxidative stress induced pyroptosis leads to osteogenic dysfunction of MG63 cells. *J Mol Histol.* **2020**;51(3):221–232.
- [28] Liang Y-B, Song -P-P, Zhu Y-H, et al. TREM-1-targeting LP17 attenuates cerebral ischemia-induced neuronal injury by inhibiting oxidative stress and pyroptosis. *Biochem Biophys Res Commun.* **2020**;529(3):554–561.
- [29] Ding X, Jian T, Wu Y, et al. Ellagic acid ameliorates oxidative stress and insulin resistance in high glucose-treated HepG2 cells via miR-223/keap1-Nrf2 pathway. *Biomed Pharmacother.* **2019**;110:85–94.
- [30] Zhang T, Wu P, Budbazar E, et al. Mitophagy reduces oxidative stress via Keap1 (Kelch-Like epichlorohydrin-associated protein 1)/Nrf2 (nuclear factor-E2-related factor 2)/PHB2 (Prohibitin 2) pathway after subarachnoid hemorrhage in rats. *Stroke.* **2019**;50(4):978–988.
- [31] Zhao MW, Yang P, Zhao LL. Chlorpyrifos activates cell pyroptosis and increases susceptibility on oxidative stress-induced toxicity by miR-181/SIRT1/PGC-1 α /Nrf2 signaling pathway in human neuroblastoma SH-

- SY5Y cells: implication for association between chlorpyrifos and Parkinson's disease. *Environ Toxicol.* **2019**;34(6):699–707.
- [32] Lu M-C, Zhao J, Liu Y-T, et al. CPUY192018, a potent inhibitor of the Keap1-Nrf2 protein-protein interaction, alleviates renal inflammation in mice by restricting oxidative stress and NF- κ B activation. *Redox Biol.* **2019**;26:101266.
- [33] Shafik NM, El-Esawy RO, Mohamed DA, et al. Regenerative effects of glycyrrhizin and/or platelet rich plasma on type-II collagen induced arthritis: targeting autophagy machinery markers, inflammation and oxidative stress. *Arch Biochem Biophys.* **2019**;675:108095.
- [34] Zhang C, Kong X, Ma D. miR-141-3p inhibits vascular smooth muscle cell proliferation and migration via regulating Keap1/Nrf2/HO-1 pathway. *IUBMB Life.* **2020**;72(10):2167–2179.
- [35] Ohta R, Tanaka N, Nakanishi K, et al. Heme oxygenase-1 modulates degeneration of the intervertebral disc after puncture in Bach 1 deficient mice. *Eur Spine J.* **2012**;21(9):1748–1757.
- [36] Li M, Huang H, Cheng F, et al. miR-141-3p promotes proliferation and metastasis of nasopharyngeal carcinoma by targeting NME1. *Adv Med Sci.* **2020**;65(2):252–258.
- [37] Donato L, Scimone C, Rinaldi C, et al. Stargardt phenotype associated with two ELOVL4 promoter variants and ELOVL4 downregulation: new possible perspective to etiopathogenesis? *Invest Ophthalmol Vis Sci.* **2018**;59(2):843–857.
- [38] Zheng C, Guo K, Chen B, et al. miR-214-5p inhibits human prostate cancer proliferation and migration through regulating CRMP5. *Cancer Biomark.* **2019**;26(2):193–202.
- [39] Hong W, Xue M, Jiang J, et al. Circular RNA circ-CPA4/ let-7 miRNA/PD-L1 axis regulates cell growth, stemness, drug resistance and immune evasion in non-small cell lung cancer (NSCLC). *J Exp Clin Cancer Res.* **2020**;39(1):149.
- [40] Ma C, Wang R, Zhao D, et al. Efficacy of platelet-rich plasma containing xenogenic adipose tissue-derived stromal cells on restoring intervertebral disc degeneration: a preclinical study in a rabbit model. *Pain Res Manag.* **2019**;6372356. DOI:10.1155/2019/6372356
- [41] Halasi M, Wang M, Chavan TS, et al. ROS inhibitor N-acetyl-L-cysteine antagonizes the activity of proteasome inhibitors. *Biochem J.* **2013**;454(2):201–208.
- [42] Li Y, Zhang L, Liu F, et al. Identification of endogenous controls for analyzing serum exosomal miRNA in patients with hepatitis B or hepatocellular carcinoma. *Dis Markers.* **2015**;893594. DOI:10.1155/2015/893594
- [43] NaPier Z, Kanim LEA, Arabi Y, et al. Omega-3 fatty acid supplementation reduces intervertebral disc degeneration. *Med Sci Monit.* **2019**;25:9531–9537.
- [44] Xie L, Huang W, Fang Z, et al. CircERC2 ameliorated intervertebral disc degeneration by regulating mitophagy and apoptosis through miR-182-5p/SIRT1 axis. *Cell Death Dis.* **2019**;10(10):751.
- [45] Cheng X, Zhang G, Zhang L, et al. Mesenchymal stem cells deliver exogenous miR-21 via exosomes to inhibit nucleus pulposus cell apoptosis and reduce intervertebral disc degeneration. *J Cell Mol Med.* **2018**;22(1):261–276.
- [46] Long J, Wang X, Du X, et al. JAG2/Notch2 inhibits intervertebral disc degeneration by modulating cell proliferation, apoptosis, and extracellular matrix. *Arthritis Res Ther.* **2019**;21(1):213.
- [47] Wang S, Ji LY, Li L, et al. Oxidative stress, autophagy and pyroptosis in the neovascularization of oxygen-induced retinopathy in mice. *Mol Med Rep.* **2019**;19(2):927–934.
- [48] Fritsch M, Günther SD, Schwarzer R, et al. Caspase-8 is the molecular switch for apoptosis, necroptosis and pyroptosis. *Nature.* **2019**;575(7784):683–687.
- [49] Donato L, Scimone C, Alibrandi S, et al. New omics-derived perspectives on retinal dystrophies: could ion channels-encoding or related genes act as modifier of pathological phenotype? *Int J Mol Sci.* **2020**;22(1):70.
- [50] Donato L, Scimone C, Alibrandi S, et al. Possible A2E mutagenic effects on rpe mitochondrial DNA from innovative RNA-Seq bioinformatics pipeline. *Antioxid (Basel).* **2020**;9(11):1158.
- [51] Scimone C, Alibrandi S, Scalinci SZ, et al. Expression of pro-angiogenic markers is enhanced by blue light in human RPE cells. *Antioxid (Basel).* **2020**;9(11):1154.